Mechanical, structural and optical properties of pristine and PVA capped zinc oxide nanocomposites

P. Gopinath[a,*], P. Suresh[b], V.Jeevanantham[c]
[a]*KSR Institute for Engineering and Technology, Tiruchengode, Namakkal -637215, Tamilnadu, India*
[b] *Mechanical Engineering at Muthayammal Engineering College, Kakkaveri, Namakkal-637408, Tamilnadu, India*
[c]*Vivekanandha College of Arts and Sciences for Women (Autonomous), Elayampalayam, Tiruchengode-637205, Tamilnadu, India*

Zinc oxide (ZnO) and Poly vinyl alcohol capped zinc oxide (PVA-ZnO) of different concentrations were synthesized by precipitation method. PVA capped ZnO nanoparticles were examined to study the influence of ZnO nanoparticles on PVA as it possesses various properties such as mechanical, structural and optical. The synthesized nanoparticles were analyzed using XRD, FTIR, UV-Vis, SEM EDAX techniques. In the FTIR spectrum, the peak observed at 559 cm^{-1} indicates M–O stretching in the samples which specifies the interaction of ZnO with PVA matrix. The XRD patterns confirmed the presence of ZnO nanoparticles and the size of the ZnO nanoparticles and PVA- ZnO NPs were 76 nm and 61 nm. The uniform dispersion of ZnO nanoparticles as well as the interaction of nanoparticles with the PVA matrix were also observed in SEM analysis and the purity of NPs was determined from EDS analysis. The UV-vis spectra show the light absorption behavior of the ZnO NPs and ZnO-PVA nanocomposites and they exhibited high absorption in the UV region. The mechanical properties such as tensile strength and elongation were also analyzed for the synthesized samples.

(Received July 6, 2021; Accepted January 6, 2023)

Keywords: Elongation, ZnO, PVA Capped ZnO, Tensile, Nanocomposites mechanical properties

1. Introduction

Zinc oxide is one among the most important group II–VI semiconductor materials. It was due to its wide direct band gap of 3.37 eV and its large excitonic binding energy of 60 meV. In general, Zinc oxide crystallized in the stable Wurtzite structure [1-2]. When in comparison to the alternative materials, ZnO had turned up an alluring material for its various properties and impressionable applications such as optoelectronic devices, reflection coatings, solar cells, anode materials, gas sensors, light emitting diodes (LED), impact on biological activities, antibacterial actions, drug delivery and so on [3-8]. Although the energy band gap of Silicon based transistors are low, it is used in many devices. So as to satisfy the disadvantages, Zinc oxide based materials were used as a thin-film transistor [9]. On account of to its broad energy band gap and high electrical properties, it was used in the optoelectronic and photovoltaic devices. When compared to GaN and Phosphorus, Zinc oxide showed high UV transmitting radiation and attained more stabilization at room temperature. Surface acoustic wave filters or SAW filters were mainly used in audio and video frequency circuits had been advanced by Zinc oxide NPs [10]. Researches had developed and reported high photoluminescence efficiencies in Zinc oxide nanostructures. In addition to that, Zinc oxide was a well-defined material where it was distinctly attractive for bio-applications. To synthesize nanomaterials, several methodologies were being used which included thermal decomposition, hydrothermal synthesis, co-precipitation, chemical vapor deposition, spin coating method etc. Among them, co-precipitation method was chosen to synthesize NPs as it was

* Corresponding author: gopipalani@ksriet.ac.in
https://doi.org/10.15251/JOR.2023.191.23

cost effective as well as stable in the environmental conditions viz., ambient temperature, pressure variance etc [11]. As a result of these properties, the synthesized NPs showed the enormous change in their shape and size as well as optical properties. Furthermore, in nano-Zinc structures, nanoparticles, nanowires the properties mentioned above could be improved well which paved the way for the upgradation of exciton oscillator quality and the quantum efficiency. The present study involved the preparation of Poly(vinylalcohol) capped Zinc oxide NPs by co-precipitation method. The goal of this work was to synthesize the NPs which indicated an extraordinary influence on optoelectronic applications. And the synthesized nanomaterials found its major usage in the preparation of novel nanomaterials with various characteristics. Only through this process of synthesis, nano-sized grain particles had been obtained with highest purity than those reported by other methods of synthesis. The prepared NPs imparted the output which could be applied in numerous applications like luminescence, optoelectronic and display devices.

2. Experimental

2.1. Materials required

PVA (C2H4O)x2 (Sigma Aldrich-Germany); Ammonium persulphate ((NH4)2S2O8, Merck, India); Zinc nitrate hexahydrate (Zn(NO3)2.6H2O, Merck, India); Sodium hydroxide (NaOH, Himedia, India); Hydrochloric acid (HCl, 37%, Loba chemicals, India). Millipore water was purchased and used as such for experiments.

2.2. Preparation of zinc oxide (ZnO)

Standard synthetic procedure for Zinc oxide NPs were reported elsewhere. To 100 ml distilled water taken in a beaker, 1M of Zinc nitrate hexahydrate ($Zn(NO_3)_2.6H_2O$) was added which formed the solution-A. To this solution-A, 2M of 100 ml Sodium hydroxide (NaOH) solution was then added drop-wise followed by vigorous stirring up to an alkaline pH of 12 was attained and stirring was continued for almost 12 hours[12]. Throughout the synthesis of NPs, the solution pH should be maintained at 12 as this seemed to be the optimum value for the formation of Zinc oxide precipitate. The precipitate thus formed had been subjected to filtration followed by washing with millipore water and ethanol. After that it was dried in oven at 100°C for about 2hrs. The dried precipitate was crumbled in an agate mortar. The same procedure should be repeated for the preparation of another samples. The powdered samples were collected and then annealing at 500°C for about two hours would be followed by stepwise cooling of 1°C /minute. To synthesize Ni-doped Zinc oxide ($Zn_{0.94}$ $Ni_{0.06}O$**)** similar procedure was pursued using stoichiometric ratios of starting precursors.

2.3. Preparation of Poly Vinyl alcohol nanocomposites

To prepare pure ZnO-PVA nanocomposites via chemical oxidative polymerization method, the following steps were involved. 1.10g of ZnO nanoparticles were dissolved in 10 ml of 1.0 mol/L HCl and the solution was added into 10.63g of vinyl alcohol monomer which was dissolved in 90 ml of 1.0 mol/L HCl and then the mixture was stirred with ultra-sonication to accelerate the dispersion. 22.82g of ammonium persulphate (APS) oxidizing agent was dissolved in 100 ml of 1.0 mol/L HCl and the solution was then added drop-wise to the mixture of ZnO nanoparticles and o- vinyl alcohol monomer solution under vigorous stirring in an ice bath for about 8–9 hours at 0–5°C. The polymeric solution slowly started to precipitate out. Finally, the formed precipitated polymer was washed with millipore water and ethanol until the filtrate became colourless, dried at oven for 12 hours at 60 °C. The final ZnO-PVA nanocomposite in base form were obtained by immersing the above HCl-doped ZnO-PVA nanocomposites into 400 ml of 1.0 mol/L $NH_3.H_2O$ solution under vigorous stirring for about 3hours at room temperature and then it was re-filtered, washed and dried. The dried dark green precipitate was collected and ground in an agate mortar and stored in desiccator for further use.

The functional group existing in the polymer and nanocomposites were characterized using Fourier Transform Infrared Spectrophotometer (FTIR), Shimadzu (Japan) in the range 4000–400 cm^{-1} with KBr pellets. The crystalline nature of the semiconductor material, polymer and

nanocomposites were characterized using X-Ray Diffraction analyzer (XRD) using X'Pert PRO, X-ray diffractometer with CuKα radiation (λ=1.5406 Å). The Scanning Electron Microscope (SEM) with JOEL, JSM and energy dispersive EDX spectrometry studies were used to analyze the surface morphology of the samples. The absorbance and reflectance of the samples were examined using UV-reflectance spectra using UV-Vis spectrophotometer model Shimadzu UV-2100. The thermal stability (TGA) of the PVA, ZnO/PVA polymeric composites were analyzed using SDT Q600 V20.9. Electrical conductance of the synthesized ZnO, PVA, ZnO/PVA polymeric composites were analyzed using four probe DC electrical conductivity instrument.

3. Results and discussion

3.1. XRD

XRD analysis was used to analyse the structure of ZnO nanoparticles, PVA polymer, and PVA capped ZnO polymeric composites which were presented in the Figure 1 [13]. From the XRD spectra, it was revealed that the PVA polymer showed a single broad peak at 2θ values around 24.5° which indicated amorphous (or) semi crystalline structure of PVA polymer since there were no sharp peaks observed, this might be due to integral factor in the XRD image. But in the XRD image of ZnO semiconductor material, it was observed that there were sharp peaks corresponding to the formation of hexagonal wurtzite structure. The peak reflections at 2θ = 31.79°, 34.37°, 36.29°, 47.59°, 56.55°, 63.21°, 66.37°, 67.86°, and 69.54° attributed to the (100), (002), (101), (102), (110), (103), (200), (112), and (201) planes which was in agreement with JCPDS no. 36-1451. When the semiconductor material was mixed with the poly vinyl alcohol, the crystalline nature diminished due to the minimal amount of semiconductor added during the synthesis of semiconductor polymeric composites which resulted in a crystalline nature. This was observed with the considerable change in the XRD image of the polymeric composites. The average particle size can be calculated using the first approximation of Debye-Scherrer formula (1),

$$D = 0.9\,\lambda/\beta\,COS\,\theta \tag{1}$$

where D is the average size of the particles, λ is the wavelength of X-ray radiation, β is the full width at half maximum intensity of the peaks, and θ is the diffraction angle [14]. From this, the particle sizes calculated for pristine ZnO and PVA Capped ZnO nanocomposites were 61 nm and 76 nm respectively.

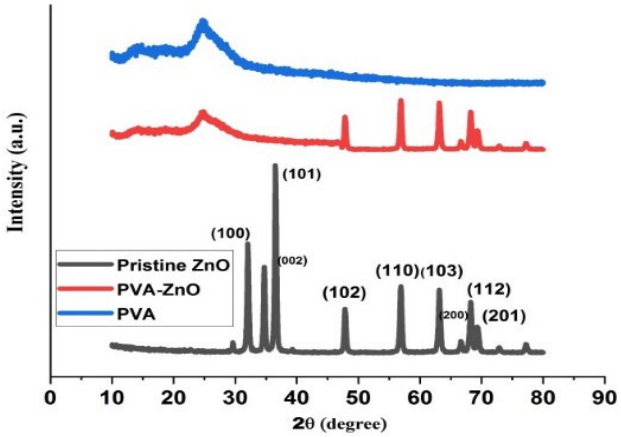

Fig. 1. XRD pattern of Synthesized pristine ZnO, PVA and PVA Capped ZnO Nanocomposites.

3.2. FTIR

The compositional properties of the prepared Pristine ZnO, PVA and PVA-ZnO nanoparticles were examined Fourier transform infrared (FTIR) spectroscopy [15]. Fourier transform infrared spectra (FT-IR) analysis is used to generate an infrared radiation absorption spectrum of a material. The characterization of Pristine ZnO, PVA and PVA-ZnO monoclinic structure in the wavenumber range 4000 − 500 cm^{-1} were shown in fig.2. The absorption peak at 559 cm^{-1} was due to M−O (ZnO) bond vibrational frequency which supports the presence of monoclinic phases. At 1149.37 cm^{-1} the sharp band was observed which corresponded to the C–O stretching of acetyl group present on the back bone of PVA. It ranges to Zn−O vibrations and formation of ZnO nanoparticles. The peak observed at 1620.44 cm^{-1} could be assigned due to C=O stretching vibration. The absorption peak observed at 3386.01 cm^{-1} was assigned to the bending and stretching vibrations of adsorbed water and surface hydroxyl group on ZnO [16]. The new bands arised might be due to the defects induced by charge transfer reaction between the polymer chain and Zinc oxide nanoparticles [17-18].

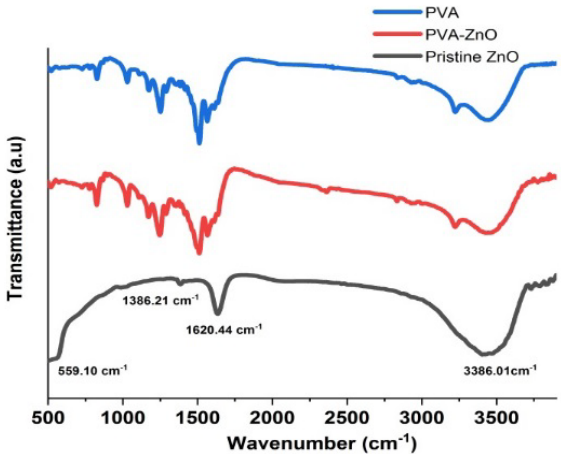

Fig. 2. FTIR Analysis of Synthesized pristine ZnO, PVA and PVA Capped ZnO.

3.3. UV-Visible

Figure 3 shows the UV-VIS absorbance spectra in the region of 200–800 nm for Pristine ZnO, PVA and PVA-ZnO nanoparticles. The absorption peaks at 374.80 nm, 390.2 nm and 393.6 nm corresponds to the Pristine ZnO, PVA and PVA-ZnO nanoparticles which was consistent with the bulk band gap of ZnO. In the absorption spectra, the peak observed at 375 nm (3.31 eV) corresponds to the exciton state in the bulk ZnO [19]. The ZnO nanoparticles showed salient exciton absorption features due to the relative large binding energy of the exciton (60 mV) although this spectrum was recorded at room temperature. From the figure it is observed that the absorption shifted gradually towards higher wavelength and exhibits a progressive redshift with the increase of incorporation of PVA into ZnO nanomaterials. The corresponding redshifts are consistent with the observed variation of the NPs sizes as reported earlier.

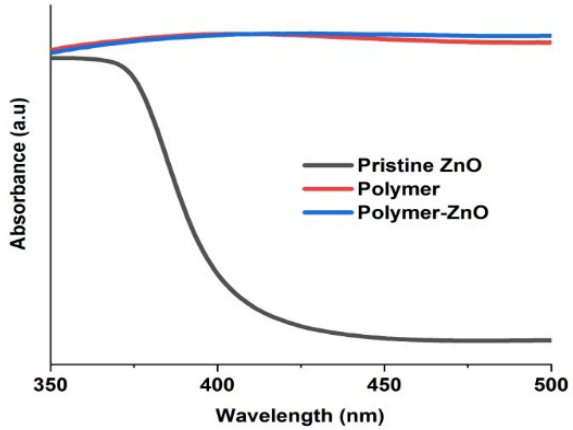

Fig. 3. UV-Visible Analysis of Synthesized pristine ZnO, PVA and PVA Capped ZnO.

3.4. SEM and EDS analysis

Scanning electron microscopy is a technique used to study the compatibility between various components of the polymer composites through the detection of phase separations and interfaces. This technique has great influence on the physical characteristics of the polymer composite. The surface morphology and the grain size of pristine ZnO, PVA and PVA-ZnO nanocomposite was shown in fig.5. The nanocomposite films exhibited uniform density of grain distribution at surface morphology [20]. The distribution of aggregates or chunks on the surface of nanocomposite films were shown by surface morphology. From this, it is concluded that, with the incorporation of ZnO on PVA polymer matrix, there is increase in aggregation of nanoparticles [21].

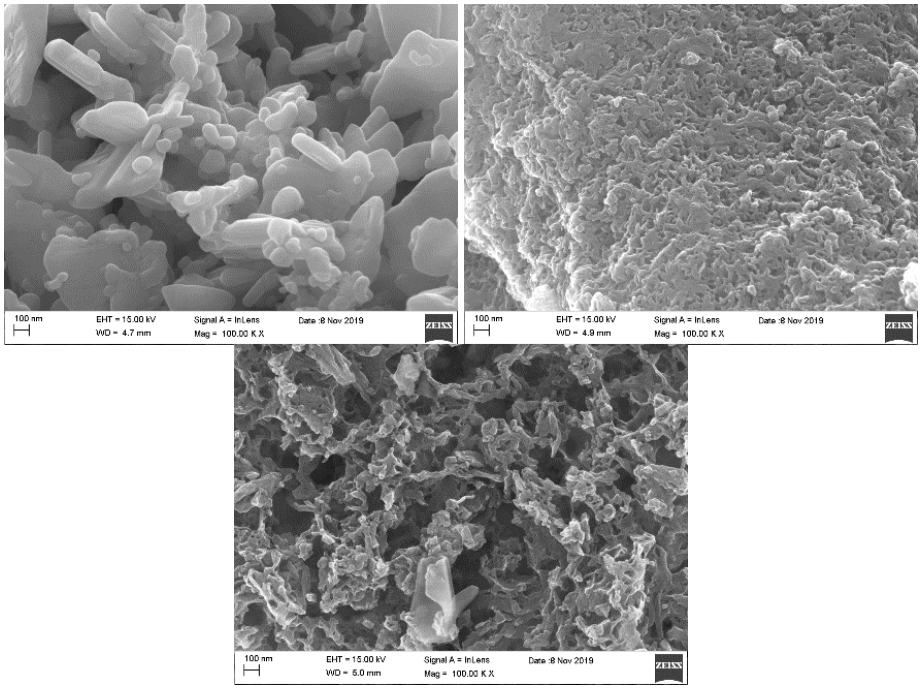

Fig. 4. SEM Analysis of Synthesized pristine ZnO, PVA and PVA Capped ZnO Nanocomposites.

The chemical composition and homogenous percentage distribution of pristine ZnO, PVA and PVA-ZnO nanocomposite were studied using energy-dispersive analysis of X-rays (EDAX) which is represented in fig.5 [22].

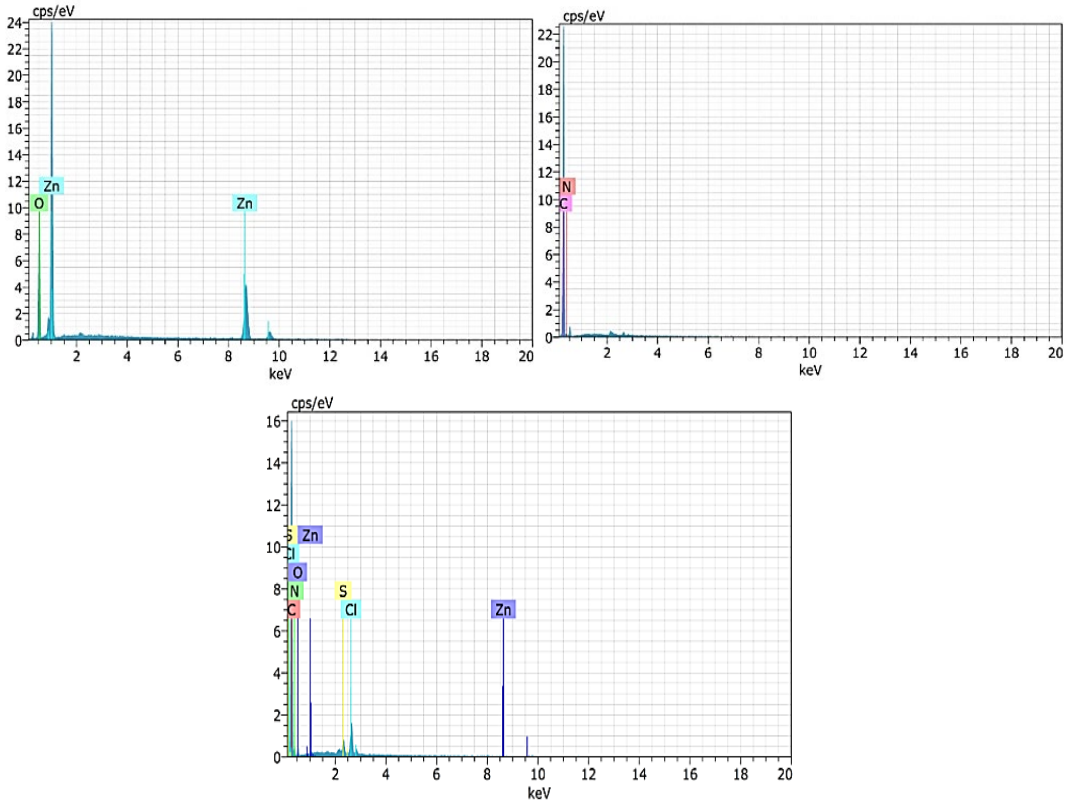

Fig. 5. EDS Analysis of Synthesized pristine ZnO, PVA and PVA Capped ZnO Nanocomposites.

3.5. Mechanical properties

The mechanical properties such as tensile strength and percentage of elongation at break (E) were estimated using UTM (universal testing-machine) - Initial grip separation (50 mm) and cross-head speed (20 mm/min) [23]. TS (Pa) and Percentage elongation {E (%)} were calculated using the following relationships (2) & (3),

$$TS = Fmax / A \tag{2}$$

where, F max is the maximum load for breaking film (N) and A is the cross-sectional area of the sample (i.e. thickness × width).

$$E(\%) = (L / L_0) \times 100 \tag{3}$$

where, L_o is the original length of the sample or initial gage length (50 mm) and L is the difference in the length at the moment of rupture. For each type of film, TS and E (%) measurements were replicated three times with individually prepared films. As the replicated experimental units and each replicate being the mean of three tested sampling units which was taken from the same film. Figure.6 denotes the plot of stress (tensile force/initial cross-sectional area) versus strain (extension as a fraction of the original length) from which tensile properties were calculated. For ZnO, PVA and PVA-ZnO nanoparticles, the mechanical properties such as tensile strength, the Young's modulus and the percentage elongation at break were investigated from the typical stress–strain curves of these materials [24]. The calculated values of TS and the Young's modulus of the film of PVA-ZnO nanoparticles were 57.33 ±3.41MPa and 1572.384±71.13MPa respectively. The percentage elongation at break of the same film was 13.99±1.47%. The TS, Young's modulus and E (%) decreases PVA-ZnO NPs than ZnO and polymer PVA. Therefore, the mechanical properties increased with increase in incorporation of PVA into ZnO matrix [25-27]. These modifications were also revealed by X-ray diffraction studies. From the table 1, it is

observed that the percentage of elongation at break increases with PVA capped ZnO nanoparticles than pristine ZnO nanoparticles.

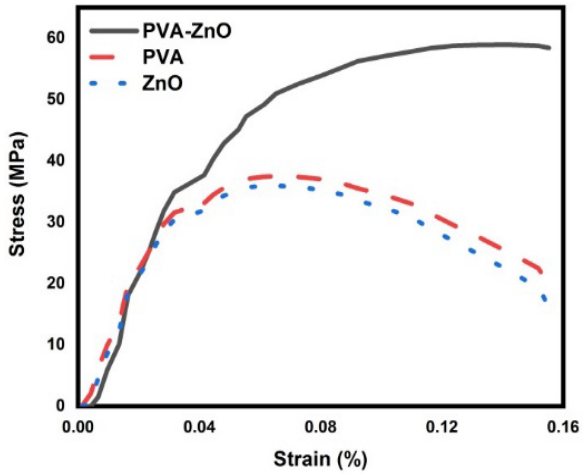

Fig. 6. Mechanical Properties of Virgin and ZnO Incorporated Polymer Films.

Table 1. Mechanical properties of synthesized materials.

Samples	TS (MPa)	YM(Mpa)	Stress(Mpa)	Elongation (%)
ZnO	44.81±3.67	1136.35±104.53	31.88	11.10±2.38
PVA	4.53±0.61	1183.54±113.86	47.89	11.44±2.19
PVA-ZnO	57.33 ±3.41	1572.384±71.13	58.63	13.99±1.47

4. Conclusion

The synthesized NPs were analyzed using FTIR, XRD and TEM studies. The absorption peak corresponds to ZnO stretching vibration (559cm−1) in the FTIR spectrum was used to confirm the functionalities present in the PVA nanocomposite. From the XRD patterns, it is concluded that ZnO NPs were in semi-crystalline phase and a broad peak observed at 24.5° revealed the presence of PVA. Further, the interaction between Zinc oxide NPs with PVA matrix was demonstrated by the existence of various crystal planes of ZnO. The particle size of pure Zinc oxide and PVA incorporated iznc oxide were found to be 61 nm and 76 nm respectively. From the scanning electron microscopy technique, it is confirmed that the nanosized ZnO particles tended to form aggregates and dispersed into the PVA polymer matrix. Also, the purity of the sample was confirmed by EDAX analysis. The absorbance of PVA nanocomposites was increased with the increase in addition of PVA into Zinc oxide nanoparticles which was confirmed by UV-vis spectral analysis. The Young's modulus and tensile strength of PVA-ZnO considerably increased when compared to the pure ZnO and PVA NPs.

References

[1] J. Duraimurugan, G. S. Kumar, M. Venkatesh et al., J Mater Sci: Mater Electron 29, 9339 (2018). https://doi.org/10.1007/s10854-018-8964-9
[2] Rai Nauman Ali, Hina Naz, Jing Li, Xingqun Zhu, Ping Liu, Bin Xiang, J. Alloys and Compounds 744, 90 (2018). https://doi.org/10.1016/j.jallcom.2018.02.072

[3] Happy Agarwal, Soumya Menon, S. Venkat Kumar, S. Rajeshkumar, Chemico-Biological Interactions 286, 60 (2018). https://doi.org/10.1016/j.cbi.2018.03.008
[4] K. S. Siddiqi, A. ur Rahman, Tajuddin et al., Nanoscale Res Lett 13, 141 (2018). https://doi.org/10.1186/s11671-018-2532-3
[5] Seungon Jung, Junghyun Lee, Jihyung Seo et al., Nano Lett. 18(2), 1337 (2018). https://doi.org/10.1021/acs.nanolett.7b05026
[6] M. Shkir, K. V. Chandekar, B. M. Alshehri et al., Appl Nanosci 10, 1811 (2020). https://doi.org/10.1007/s13204-019-01236-6
[7] Harshini Muthukumar, Samsudeen Naina Mohammed, Nivedhinilswarya Chandrasekaran et al., Int. J. Hydrogrn Energy 44(4), 2407 (2019). https://doi.org/10.1016/j.ijhydene.2018.06.046
[8] Diben Wu, Huijie Wu, Yubin Niu, Chao Wang, Zhuan Chen et al., Powder Technology 367, 774 (2020). https://doi.org/10.1016/j.powtec.2020.04.046
[9] Qian Zhang, Guodong Xia, Lubin Li, Wenwen Xia, Hongyu Gong, Sumei Wang, Current Applied Physics 19(2), 174 (2019). https://doi.org/10.1016/j.cap.2018.10.012
[10] S Satheeskumar, V Jeevanantham, D Tamilselvi, J. Ovon. Res 14,154 (2018)
[11] Khairul Basyar Baharudin, Nurulhuda Abdullah,Darfizzi Derawi, Mater. Res. Express 5, 125018 (2018). https://doi.org/10.1088/2053-1591/aae243
[12] Shabnam Fakhari, Mina Jamzad, Hassan Kabiri Fard, Green Chemistry Letters and Reviews 12(1), 19 (2019). https://doi.org/10.1080/17518253.2018.1547925
[13] A. Azmi, K. S. Lau, S. X. Chin et al. Cellulose 28, 2241 (2021). https://doi.org/10.1007/s10570-021-03695-z
[14] O. O. Balayeva, A. A. Azizov, M. B. Muradov, R. M. Alosmanov, G. Q. Mursalova, K. S. Rahimli, Z. A. Aghamaliyev, Journal of Dispersion Science and Technology, 1 (2020). https://doi.org/10.1080/01932691.2020.1773848
[15] V. Jeevanantham, K. Hemalatha, S. Satheeskumar Journal of Ovonic Research 14, 269 (2018)
[16] Saengnapa Kakarndee, Suwat Nanan, Journal of Environmental Chemical Engineering 6(1), 74 (2018). https://doi.org/10.1016/j.jece.2017.11.066
[17] Aswathy Jayakumar, Sabarish Radoor, Indu C. Nair, Suchart Siengchin et al., Process Biochemistry, 102 (2021). https://doi.org/10.1016/j.procbio.2020.12.010
[18] Shadpour Mallakpour, Elaheh Shafiee, Ultra Sonics Sonochemistry 40(A), 881 (2018). https://doi.org/10.1016/j.ultsonch.2017.08.039
[19] Palani Gopinath, Paramasivam Suresh, Materials Science (Medžiagotyra), 28, 236 (2022) https://doi.org/10.5755/j02.ms.28608
[20] Rong Zhang, Yihao Wang, Donghui Ma, Saeed Ahmed, Wen Qin, Yaowen Liu, Ultrasonics Sonochemistry 59, 104731 (2019). https://doi.org/10.1016/j.ultsonch.2019.104731
[21] Alireza Khalilipour, Azin Paydayesh, Journal of Macromolecular Science Part B, 2019.
[22] M. Aslam, M. A. Kalyar, Z. A. Raza, Journal of Elec Materi 47, 3912 (2018). https://doi.org/10.1007/s11664-018-6270-1
[23] Rong Zhang, Yihao Wang, Donghui Ma, Saeed Ahmed et al., Ultrasonics Sonochemistry 59, 104731 (2019). https://doi.org/10.1016/j.ultsonch.2019.104731
[24] Ahmed Gamal El-Shamy, Progress in Organic Coatings 150, 105981 (2021). https://doi.org/10.1016/j.porgcoat.2020.105981
[25] Maryam Azizi-Lalabadi, Mahmood Alizadeh-Sani, Baharak Divband, Ali Ehsani, David Julian McClements, Food Research International 137, 109716 (2020). https://doi.org/10.1016/j.foodres.2020.109716
[26] A Panneerselvam, J Velayutham, S Ramasamy, IET nanobiotechnology 15 (2), 164-172 (2021) https://doi.org/10.1049/nbt2.12033
[27] S Arul, T Senthilnathan, V Jeevanantham, KV Satheesh Kumar, Archives of Metallurgy and Material,11 66 (2021)